Electrochemical oxidation of crystal violet using a BDD anode with a solid polymer electrolyte

Nizar Klidi[a], Davide Clematis[b], Maria Paola Carpanese[b,] Abdellatif Gadri[a], Salah Ammar[a] and Marco Panizza[b,*]

[a] *Unité de Recherche Electrochimie, Matériaux et Environnement UREME (UR17ES45), Faculté des Sciences de Gabès, Université de Gabès, Cité Erriadh, 6072 Gabès, Tunisie*

[b] *Department of Civil, Chemical and Environmental Engineering, University of Genoa, P. le J.F. Kennedy 1 – 16129 Genova, Italy*

Abstract

This paper explores the applicability of an innovative electrochemical cell with a solid polymer electrolyte (SPE) with mesh electrodes for the electrochemical oxidation of a low conductivity solution (0.022 mS/cm) containing crystal violet (CV) dye compound as model pollutant in a range concentration of 25-100 mg/L. The system anode/membrane/cathode is formed by Nafion membrane sandwiched between a Ti/RuO_2 cathode and a BDD anode. The dependence of applied current, stirring rate, supporting electrolyte and temperature has been investigated. The experimental results showed that the electrochemical cell with SPE is suitable for the treatment of solution with a very low conductivity since the CV solution was completely mineralized with an energy consumption of about 60 kWh m^{-3}. Furthermore, the process was under charge transfer control for low applied current, becoming mass transfer control around 1 A. The addition of supporting electrolyte as Na_2SO_4 (0.6 and 1 g/L) and $NaHCO_3$ (1 g/L) to the solution decreased the removal rate due to the presence of competitive reaction and scavengers media. The evolution of nitrogen compounds during the electrolysis shows that at the end of the process the 80% of initial N has been converted in nitrate and ammonium, indicating the formation of volatile compound.

Keywords: diamond electrode; direct electrolysis; solid polymer electrolyte; crystal violet; low conductivity.

1. Introduction

Wastewater treatment is one of the currently most important challenge under a technological and economical point of view. The development of processes able to remove the highest amounts of pollutants, reducing sludge and costs is a key factor. Classical treatments, such as biological and chemical approaches, have shown their limits, mostly as regards the high production of sludge, which can require a special disposal. One possible solution is offer by electrochemical technologies, in particular by electrochemical advanced oxidation processes (EAOPs) that allow the treatment of several kind of residuals (pharmaceutical, textile, urban and industrial) also containing persistent pollutants [1-4]. A wide range of electrochemical processes have been developed for the treatment of effluents and the most studied are the anodic oxidation with BDD electrode [5-9] and electro-Fenton processes [10-14]. Their suitability for organic recalcitrant compounds removal is due to the production of a strong oxidative reagent, the hydroxyl radicals ($^{\bullet}OH$). EAOPs appeal is also supported by different factors among which the possibility to operate at ambient temperature and pressure, easier management than conventional technology, and their scalability. Furthermore, the main operating variables allow a better and reliable cost evaluation.

The improvement of economic feasibility of electrochemical treatments is crucial and one fundamental parameter to define the energy consumption is the solution conductivity. In fact, the long treatment time typically required by electrochemical methods make the conductivity closely related with the running cost of the industry. The increase of conductivity leads to a lower voltage losses and energy consumption. Nevertheless, residual from different productive sectors (e.g. pharmaceutical industries, food industries, hospital wastewaters, etc.) do not fulfill the high conductivity solution condition. To get over the restriction due to the conductivity and to provide a rapid oxidation of pollutants with high current efficiencies different approaches have been proposed such as the adoption of capillary cells, the use of microfluidic cells [15-17], the addition of an excess of a supporting electrolyte or the employment of a solid polymer electrolyte (SPE). Up to now the addition of a supporting electrolyte (Na_2SO_4, $NaCl$, $NaClO_4$, etc.) is the most used technique, due to its efficacy and easiness but there are relevant problems such as the cost of the electrolyte and the authorization procedure and the possible formation of persistent by-products toxic for environmental, especially in presence of Cl^- and SO_4^- ions.

2

Considering these aspects, the SPE solution, in which a solid polymer electrolyte is placed between anode and cathode, has received a great attention and technological development, guaranteeing an adequate current flux in a solution with low conductivity, with promising removing results. Possible drawbacks of its employment are the cost of membrane and possible formation of fouling. Currently, in electrochemical industry, solid polymer is especially employed to produce ozone [18-24] but it can be effectively used in electrochemical processes for wastewaters treatment [25-28].

For example, Kraft et al. [26] demonstrated that benzyl alcohol can be successfully mineralized in aqueous solutions with very low ionic conductivity using a diamond electrode/polymer electrolyte/diamond electrode SPE sandwiches. Recently, Clematis et al. [28] reported on the application of SPE for the oxidation of Safranin T in aqueous solution with low conductivity, obtaining the complete removal of the dye and the reduction of the COD of the solution to zero.

In this article, the oxidation of synthetic solution with low conductivity containing crystal violet (CV) as model organic compound was investigated using a Nafion® membrane as solid polymer electrolyte in order to optimize the experimental conditions and reduce the energy consumption. The membrane was sandwiched between a boron-doped diamond (BDD) anode and a Ti/RuO_2 cathode. The BDD anode was selected as anode material for its ability to oxidize a wide range of pollutants, as reported in many previous papers [29-36]. The choice of CV as model compound to evaluate the applicability of SPE has been made because it can be present in hospital wastewater, which usually presents a low conductivity. It is commonly used in the Gramm stain technique for differentiation of Gram-negative versus Gram-positive bacteria.

2. Experimental

2.1. Chemicals

The synthetic solution was made by dissolving 50 mg/L of CV ($C_{25}H_{30}N_3Cl$, Sigma Aldrich with purity >90%) in tap water (0.29 mS/cm) or in double distilled water (0.022 mS/cm). In some experiments, 0.6 g/L of Na_2SO_4 (0.85 mS/cm), 1 g/L of Na_2SO_4 (1.2 mS/cm) or 1 g/L of $NaHCO_3$ (0.83 mS/cm) were added to the double distilled water. Na_2SO_4 and $NaHCO_3$ were analytical grade from Sigma Aldrich.

2.2. Electrolytic system

All electrolyses were carried out in an open, undivided, cylindrical glass cell containing 500 mL solutions under stirring by a magnetic bar with an adjustable rotation speed. The stirring ranging between 100 and 1100 rpm, that corresponds to mass transfer coefficient k_m between $3.8 \times 10^{-6} \div 1.9 \times 10^{-5}$ m s^{-1}. Electrolysis operate, in galvanostatic condition using an AMEL 2055 potentiostat/galvanostat.

Anode/membrane/cathode sandwiches were constructed by sandwiching a Nafion® N324 ion exchange membranes between a Nb/BDD mesh anode and a Ti/RuO$_2$ mesh cathode, as presented in Figure 1. The geometrical area of the electrodes was 3.5 cm 7.5 cm and they were separated by a distance of 0.15 mm. The diamond electrodes were purchased from

Condias and are DIACHEM® mesh electrodes with a diamond film of about 5 μm. The

doping level of boron in the diamond layer expressed as boron/carbon ratio was about 3500 ppm deposited on a niobium substrate 1.5 mm thick with six boreholes diameter 4.5 mm. The Ti/RuO$_2$ cathode was purchased from De Nora industries. More details on the electrochemical cell were given elsewhere [28].

2.3. Analysis

The degradation of CV was followed by spectrophotometric measurements using a JASCO V 630 spectrophotometer with cells a 1 cm path length. The Total Organic Carbon (TOC) of the initial solution and electrolyzed sample was evaluated with a Dr. Lange DR3900 system. Chemical analyses of the water-soluble inorganic ions (NH_4^+, NO_2^- and NO_3^-) were performed using Ion Chromatography (Metrohm 761 Compact IC, Switzerland) equipped with a guard precolumn and a conductivity detector.

The mineralization current efficiency (MCE in %) for each treated solution at a given electrolyses time t (h) was then calculated from TOC values, using the following relationship [37]:

$$\tag{1}$$

where n is the number of electrons consumed in the mineralization process of each VC molecule, F is the Faraday constant (96487 C mol^{-1}), V_s is the solution volume (dm^3), $\Delta(TOC)_{exp}$ is the experimental TOC decay (mg dm^{-3}), 4.32×10^7 is a conversion factor (3600 s h^{-1} ×12000 mg of C mol^{-1}), m is the number of carbon atoms in a CV molecule and I is the applied current (A).

The number of electrons (n) exchanged per each CV molecule was taken as 129 because its total mineralization involves complete conversion into carbon dioxide, chlorides, ammonium and nitrates as main ions, as will be discussed below, following reaction (2):

$$C_{25}H_{30}N_3Cl + 53H_2O \rightarrow 25CO_2 + 2NH_4^+ + NO_3^- + 128H^+ + Cl^- + 129e^- \tag{2}$$
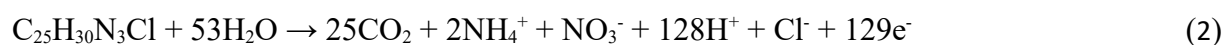
The specific energy consumption (, in kWh m^{-3}) was calculated as follows [38]:

$$\tag{3}$$

Where U_{cell} is the cell potential (V), t is the duration of the electrolysis (s), I is the applied current (A), V is the volume of the solution (dm^3).

3. Results and discussion

3.1. Influence of applied current

The applied current intensity is one of the parameters that influence the electrochemical oxidation of organic pollutant. To find the adequate operating conditions for the degradation of CV by the electrochemical oxidation method, a series of experiments were realized using different current intensity ranging from 0.5 A to 1.5 A during 100 min of electrolysis time.

Figure 2 shows that the complete removal of 50 mg/L of CV was obtained in all experiments, thanks to the reaction of CV with the electrogenerated ·OH radicals according to Eq. (4):

$$H_2O \rightarrow {}^\bullet OH + H^+ + e^- \tag{4}$$

An increase of the applied current from 0.5 A to 1.0 A favoured the oxidation of the dye and the electrolysis time for the complete CV removal decreased from 100 to 70 min, due to the greater production of hydroxyl radicals.

On the contrary, a further increase of the current at 1.5 A did not produced significant improvements in the oxidation rate. This fact indicates that at low currents, the oxidation is under charge transfer control, while at higher currents the process became controlled by mass-

transport and an increase of the applied current does not favored the oxidation of the pollutants but increase the secondary oxygen evolution [39]:

$$2H_2O \rightarrow O_2 + 4H^+ + 4e^- \tag{5}$$

The effect of reaction (5) is also observable considering the CV removal as a function of charge Q (Ah L^{-1}), as reported in the inset of Fig. 2. Up to applied current equal to 1 A the specific charge required is 1.66 Ah L^{-1}, while increase to 2 Ah L^{-1} for an applied current of 1.5 A.

Moreover, an increase of the applied current resulted also in an increase of the cell potential that was 8.1 V, 8.7 V and 9.8 V at 0.5 A, 1 A and 1.5 A, respectively. The energy consumption for the removal of 97% of CV was 13.5 kWh m^{-3}, 14.5 kWh m^{-3} and 19.6 kWh m^{-3} at 0.5 A, 1 A and 1.5 A, respectively.

3.2. Influence of stirring rate

In order to better understand the effect of the mass transfer of the oxidation of CV, some electrolyses were performed at 1 A with four stirring rates in the range 100 – 1100 rpm and the results are presented in Figure 3. As can be seen, the time necessary for the complete CV removal significantly decreased with increasing the stirring rate from 100 to 800 rpm (k_m from 3.8×10^{-6} m s^{-1} to 1.9×10^{-5} m s^{-1}), meaning that at 1 A the oxidation is mainly controlled by the mass transport of the pollutants towards the electrode surface. On the contrary, at very high stirring rate, e.g. 1100 rpm (1.9×10^{-5} m s^{-1}), no significant improvements were obtained because in these conditions, many bubbles were produced during the stirring of the solution and probably they decreased the active surface of the electrodes.

3.3. Effect of the electrolyte support type and concentration

Figure 4 compares the CV removal during electrolysis at different electrolytes. The test carried out in tap water (i.e. 174 mg/L of bicarbonates, 15 mg/L of sulphates, 3 mg/L of nitrates and 1.2 mg/L of chlorides) does not show big differences from the experiment performed in double distilled water. These results indicate that the oxidation rate is not considerably influenced by the very low concentration of inorganic ions in tap wastewater.

To evaluate the effect of higher concentration of supporting electrolyte, different amounts of Na_2SO_4 (0.6 g/L or 1 g/L) or $NaHCO_3$ (1 g/L) were added to the distilled water. Their presence decreased the removal rate, and the time necessary to remove 95% of CV was 100 and 60 min with addition of 1 g/L of Na_2SO_4 and 1 g/L of $NaHCO_3$, respectively.

6

Na$_2$SO$_4$ effect can be explained by the high oxidation power of BDD anode surface, that allows the competitive and parallel production of several side products, such as peroxodisulphates generated by the oxidation of sulphates (reaction 4) [40, 41]

$$2SO_4^{2-} \rightarrow S_2O_8^{2-} + 2e^- \qquad (6)$$

Persulfates are strong oxidants at high temperature, but at 20 °C they have lower oxidation potential than $^\bullet$OH radicals and consequently the removal rate decreased in the presence of sulphates, with a depletion of hydroxyl radicals. The negative impact of sulfate medium has been deeply investigated by Zhang et al. [42]. In this paper was detected that using a BDD anode a SO$_4^{2-}$ concentration lower than 50 mM lead to a worsening of the performance removal due to the reasons introduced above.

As regard HCO$_3^-$, its presence can reduce reaction rate and inhibit CV oxidation, due to a scavengers action on hydroxyls radicals as reported by different papers [40, 43].

However, the addition of supporting electrolyte also has the advantage of lowering of the cell potential. For example, the cell potential was 8.7 V in double distilled water, 8.5 V in tap water, 8.0 V in 1 g/L NaHCO$_3$, 7.6 V in 0.6 g/L Na$_2$SO$_4$ and 7.1 V in 1 g/L Na$_2$SO$_4$. Consequently, the specific energy consumption for the removal of 97% of CV was 14.5 kWh m^{-3} in double distilled water, 17.2 kWh m^{-3} tap water, 21.3 kWh m^{-3} in 1 g/L NaHCO$_3$, 24.8 kWh m^{-3} in 0.6 g/L Na$_2$SO$_4$ and 23.6 kWh m^{-3} in 1 g/L Na$_2$SO$_4$.

3.4. Effect of the concentration of crystal violet and temperature

Figure 5 shows the influence of the initial concentration of CV and temperature on the dye removal during the electrolysis at 1 A and 800 rpm. Regarding the effect of initial dye content, overall degradation was obtained in all cases but the time for the complete removal increased with initial CV concentration due to the presence of a greater amount of organics in the medium. Taking into account a pseudo-first order reaction kinetic, the apparent rate constants were calculated as shown in Fig. 5 inset; the higher is the initial polluting load the lower is the kinetic constant (from 0.097 s^{-1} at 25 ppm to 0.041 s^{-1} at 100 ppm). The main cause of this reaction rate drop is the enhancement of competitive reactions, which involved intermediate compounds formed and hydroxyl radicals.

After 30 min, for example, CV was reduced by 94%, 87% and 63%, proving a gradual loss in percentage of CV removal when rising the initial concentration from 25 to 100 mg/L. Nevertheless, an increase in dye content accelerates the CV removal rate (the amount of dye that is removed per time period), owing to the decrease in the mass-transport limitation. In

fact, after 30 min, for example, 23.5, 43.5 and 36 mg/L of CV were already oxidized from starting solutions containing 25, 50 and 100 mg/L of dye, respectively.

Figure 5 also shows that CV removal rate was not affected by the temperature in the range 20 °C to 50 °C.

3.6. Mineralization and release of inorganic ions

In order to verify the effectiveness of the SPE cell for the mineralization of the CV, an electrolysis was performed at 1.0 A with a stirring rate of 800 rpm at 20 °C and the TOC of the solution was monitored during the oxidation.

Figure 6a shows that after 240 min, the TOC was almost completely removed, meaning that the solution was mineralized to CO_2 and water according to the equation (2). The faster removal of CV concentration (expressed in term of mg/L of carbon) compared to the removal of TOC indicated that some oxidation intermediates are formed during the electrolysis. The evolution of the concentration of these compounds obtained by the difference between TOC and CV concentration, increased in the first 30 min and then it progressively decreased up to zero. The MCE (Figure 6a, inset) reached a maximum of 25% at 20 min, and then it progressively decays during treatment reaching 5% at 240 min. This pattern can be related to gradual organic concentration decrease in the solution and consequently to an increase of the secondary oxygen evolution (Eq. 5) because the oxidation was under mass transport control.

Figure 6b shows the evolution of nitrogenated ions released during the oxidation. Ammonium was formed as cation; nitrate was the accumulated anions, whereas no NO_2^- were detected. As can be seen, a quick accumulation of NO_3^- was obtained and it reached a steady concentration of about 0.095 mM NO_3^- (corresponding to 25% of initial N). A more gradual accumulation was achieved for ammonium and after 240 min of electrolysis, 0.205 mM NH_4^+ (corresponding to 55% of initial N) and were found. The sum of nitrate + ammonium ions accounted for by 80% of initial N contained in CV and hence, some volatile N-species were plausibly formed during the electrolyses.

3.7. Energy consumption

One of the key parameters for electrochemical process, which requires an investigation and optimization, is the energy consumption ($kWhm^{-3}$), calculated from Eq. (1). The evolution of specific energy consumptions as function of TOC abatement and CV removal were investigated in the best operating conditions found previously (applied current 1 A; electrolyte: double distilled water; stirring rate: 800 rpm; T = 20°C) and the result are presented in Figure 7. The specific energy consumption increases slowly for TOC and CV

removal lower than 70% and later it has a sharp increase, especially for TOC. In fact, when the content of the organic pollutants became very low, the oxidation became strongly limited by the mass-transport and the main anodic reaction was the oxygen evolution (Eq. 5) and consequently the specific energy consumption increased. However, the complete mineralization of the solution required about 60 kWh m^{-3} that is an acceptable value if we consider that the solution has very low conductivity, while the CV degradation required 15 kWh m^{-3}.

4. Conclusions

The sandwich BDD anode/Nafion/TiRuO$_2$ cathode cell setup has been successfully used on the oxidation of CV in aqueous solution. Electrolysis studies showed that this method can completely remove CV and almost the TOC of the solution.

Results show that the process was under charge transfer control for low applied current, becoming mass transfer control around 1 A. This conclusion has been also supported by experiments performed at different stirring rate in the range of 100-1100 rpm and an applied current of 1 A.

The presence of supported electrolyte as a strong influence on CV removal, increasing the necessary time to obtain a complete oxidation of pollutant, due to the presence of competitive reaction and scavengers media.

The evolution of nitrogen compounds during the electrolysis shows that at the end of the process the 80% of initial N has been converted in nitrate and ammonium, indicating the formation of volatile compound.

A further confirmation that the sandwich system with SPE is suitable for the treatment of solution with a very low conductivity has been obtained from energy consumption analysis, which indicate an energy demand about 60 kWh m^{-3}, acceptable for these conductivity values.

References

[1] C.A. Martínez-Huitle, M.A. Rodrigo, I. Sirés, O. Scialdone, Single and Coupled Electrochemical Processes and Reactors for the Abatement of Organic Water Pollutants: A Critical Review, Chem. Rev., 115 (2015) 13362-13407.

[2] M. Panizza, G. Cerisola, Direct And Mediated Anodic Oxidation of Organic Pollutants, Chem. Rev., 109 (2009) 6541-6569.

[3] I. Sires, E. Brillas, M.A. Oturan, M.A. Rodrigo, M. Panizza, Electrochemical advanced oxidation processes: today and tomorrow. A review, Environ. Sci. Pollut. Res. Int., 21 (2014) 8336-8367.

[4] G. Chen, Electrochemical technologies in wastewater treatment, Sep. Purif. Technol., 38 (2004) 11-41.

[5] M. Panizza, G. Cerisola, Application of diamond electrodes to electrochemical processes, Electrochim Acta, 51 (2005) 191-199.

[6] L. Labiadh, A. Barbucci, M.P. Carpanese, A. Gadri, S. Ammar, M. Panizza, Comparative depollution of Methyl Orange aqueous solutions by electrochemical incineration using TiRuSnO$_2$, BDD and PbO$_2$ as high oxidation power anodes, J. Electroanal. Chem., 766 (2016) 94-99.

[7] M. Panizza, D. Clematis, G. Cerisola, Electrochemical treatment of poorly biodegradable DPC cationic surfactant, J. Environ. Chem. Eng., 4 (2016) 2692-2697.

[8] H. Rubí-Juárez, S. Cotillas, C. Sáez, P. Cañizares, C. Barrera-Díaz, M.A. Rodrigo, Use of conductive diamond photo-electrochemical oxidation for the removal of pesticide glyphosate, Sep. Purif. Technol., 167 (2016) 127-135.

[9] M.S. Çelebi, N. Oturan, H. Zazou, M. Hamdani, M.A. Oturan, Electrochemical oxidation of carbaryl on platinum and boron-doped diamond anodes using electro-Fenton technology, Sep Purif Technol, 156, Part 3 (2015) 996-1002.

[10] E. Brillas, I. Sirés, M.A. Oturan, Electro-Fenton Process and Related Electrochemical Technologies Based on Fenton's Reaction Chemistry, Chem. Rev., 109 (2009) 6570-6631.

[11] L. Labiadh, M.A. Oturan, M. Panizza, N.B. Hamadi, S. Ammar, Complete removal of AHPS synthetic dye from water using new electro-fenton oxidation catalyzed by natural pyrite as heterogeneous catalyst, J. Hazard. Mater., 297 (2015) 34-41.

[12] H. Olvera-Vargas, N. Oturan, M.A. Oturan, E. Brillas, Electro-Fenton and solar photoelectro-Fenton treatments of the pharmaceutical ranitidine in pre-pilot flow plant scale, Sep Purif Technol, 146 (2015) 127-135.

[13] I. Sirés, C. Arias, P.L. Cabot, F. Centellas, J.A. Garrido, R.M. Rodríguez, E. Brillas, Degradation of clofibric acid in acidic aqueous medium by electro-Fenton and photoelectro-Fenton, Chemosphere, 66 (2007) 1660-1669.

[14] I. Sirés, N. Oturan, M.A. Oturan, R.M. Rodríguez, J.A. Garrido, E. Brillas, Electro-Fenton degradation of antimicrobials triclosan and triclocarban, Electrochim Acta, 52 (2007) 5493-5503.

[15] P. Ma, H. Ma, S. Sabatino, A. Galia, O. Scialdone, Electrochemical treatment of real wastewater. Part 1: Effluents with low conductivity, Chem. Eng. J., 336 (2018) 133-140.

[16] S. Sabatino, A. Galia, O. Scialdone, Electrochemical abatement of organic pollutants in continuous-reaction systems through the assembly of microfluidic cells in series, ChemElectroChem, 3 (2016) 83-90.

[17] O. Scialdone, C. Guarisco, A. Galia, Oxidation of organics in water in microfluidic electrochemical reactors: Theoretical model and experiments, Electrochim. Acta, 58 (2011) 463-473.

[18] K. Arihara, C. Terashima, A. Fujishima, Electrochemical Production of High-Concentration Ozone-Water Using Freestanding Perforated Diamond Electrodes, J. Electrochem. Soc., 154 (2007) E71.

[19] Y. Cui, Y. Wang, B. Wang, H. Zhou, K.-Y. Chan, X.-Y. Li, Electrochemical Generation of Ozone in a Membrane Electrode Assembly Cell with Convective Flow, J. Electrochem. Soc., 156 (2009) E75.

[20] L.M. Da Silva, D.V. Franco, L.G. Sousa, I.C. Gonçalves, Characterization of an electrochemical reactor for the ozone production in electrolyte-free water, J. Appl. Electrochem., 40 (2010) 855-864.

[21] A.V. Diniz, N.G. Ferreira, E.J. Corat, V.J. Trava-Airoldi, Efficiency study of perforated diamond electrodes for organic compounds oxidation process, Diam. Relat. Mater., 12 (2003) 577-582.

[22] Y. Honda, T.A. Ivandini, T. Watanabe, K. Murata, Y. Einaga, An electrolyte-free system for ozone generation using heavily boron-doped diamond electrodes, Diam. Relat. Mater., 40 (2013) 7-11.

[23] F. Okada, K. Naya, Highly Efficient and Long-Lifetime Ozone Water Production System Realized Using a Felt Separator, J. Electrochem. Soc., 156 (2009) E125.

[24] K. Onda, T. Ohba, H. Kusunoki, S. Takezawa, D. Sunakawa, T. Araki, Improving Characteristics of Ozone Water Production with Multilayer Electrodes and Operating

Conditions in a Polymer Electrolyte Water Electrolysis Cell, J. Electrochem. Soc., 152 (2005) D177.

[25] O. Simond, C. Comninellis, Anodic oxidation of organics on Ti/IrO$_2$ anodes using Nafion as electrolyte, Electrochim. Acta, 42 (1997) 2013-2018.

[26] A. Kraft, M. Stadelmann, M. Wünsche, M. Blaschke, Electrochemical destruction of organic substances in deionized water using diamond anodes and a solid polymer electrolyte, Electrochem. Commun., 8 (2006) 155-158.

[27] K. Zakaria, P.A. Christensen, The Use of Ni/Sb–SnO$_2$-based Membrane Electrode Assembly for Electrochemical Generation of Ozone and the Decolourisation of Reactive Blue 50 Dye Solutions, Electrochim. Acta, 135 (2014) 11-18.

[28] D. Clematis, G. Cerisola, M. Panizza, Electrochemical oxidation of a synthetic dye using a BDD anode with a solid polymer electrolyte, Electrochem. Commun., 75 (2017) 21-24.

[29] N. Flores, P.L. Cabot, F. Centellas, J.A. Garrido, R.M. Rodríguez, E. Brillas, I. Sirés, 4-Hydroxyphenylacetic acid oxidation in sulfate and real olive oil mill wastewater by electrochemical advanced processes with a boron-doped diamond anode, J. Hazard. Mater., 321 (2017) 566-575.

[30] A. Bedolla-Guzman, I. Sirés, A. Thiam, J.M. Peralta-Hernández, S. Gutiérrez-Granados, E. Brillas, Application of anodic oxidation, electro-Fenton and UVA photoelectro-Fenton to decolorize and mineralize acidic solutions of Reactive Yellow 160 azo dye, Electrochim. Acta, 206 (2016) 307-316.

[31] J. Llanos, S. Cotillas, P. Cañizares, M.A. Rodrigo, Conductive diamond sono-electrochemical disinfection (CDSED) for municipal wastewater reclamation, Ultrason. Sonochem., 22 (2015) 493-498.

[32] A.S. Fajardo, R.C. Martins, C.A. Martínez-Huitle, R.M. Quinta-Ferreira, Treatment of Amaranth dye in aqueous solution by using one cell or two cells in series with active and non-active anodes, Electrochim. Acta, 210 (2016) 96-104.

[33] A. Kapaka, G. Foti, C. Comninellis, Kinetic modelling of the electrochemical mineralization of organic pollutants for wastewater treatment, J. Appl. Electrochem., 38 (2008) 7-16.

[34] Á. Anglada, A. Urtiaga, I. Ortiz, D. Mantzavinos, E. Diamadopoulos, Boron-doped diamond anodic treatment of landfill leachate: Evaluation of operating variables and formation of oxidation by-products, Water Res., 45 (2011) 828-838.

[35] O. Scialdone, A. Galia, S. Randazzo, Oxidation of carboxylic acids in water at IrO_2–Ta_2O_5 and boron doped diamond anodes, Chem. Eng. J., 174 (2011) 266-274.

[36] M. Mascia, A. Vacca, A.M. Polcaro, S. Palmas, J.R. Ruiz, A. Da Pozzo, Electrochemical treatment of phenolic waters in presence of chloride with boron-doped diamond (BDD) anodes: Experimental study and mathematical model, J. Hazard. Mater., 174 (2010) 314-322.

[37] M. Panizza, M.A. Oturan, Degradation of Alizarin Red by electro-Fenton process using a graphite-felt cathode, Electrochim Acta, 56 (2011) 7084-7087.

[38] M. Panizza, A. Barbucci, M. Delucchi, M.P. Carpanese, A. Giuliano, M. Cataldo-Hernández, G. Cerisola, Electro-Fenton degradation of anionic surfactants, Sep. Purif. Technol., 118 (2013) 394-398.

[39] S.C. Elaoud, M. Panizza, G. Cerisola, T. Mhiri, Electrochemical degradation of sinapinic acid on a BDD anode, Desalination, 272 (2011) 148-153.

[40] R.E. Palma-Goyes, F.L. Guzmán-Duque, G. Peñuela, I. González, J.L. Nava, R.A. Torres-Palma, Electrochemical degradation of crystal violet with BDD electrodes: Effect of electrochemical parameters and identification of organic by-products, Chemosphere, 81 (2010) 26-32.

[41] A. El-Ghenymy, F. Centellas, R.M. Rodríguez, P.L. Cabot, J.A. Garrido, I. Sirés, E. Brillas, Comparative use of anodic oxidation, electro-Fenton and photoelectro-Fenton with Pt or boron-doped diamond anode to decolorize and mineralize Malachite Green oxalate dye, Electrochim. Acta, 182 (2015) 247-256.

[42] C. Zhang, Z. He, J. Wu, D. Fu, The peculiar roles of sulfate electrolytes in BDD anode cells, J. Electrochem. Soc., 162 (2015) E85-E89.

[43] Y. Li, S. Yang, C. Sun, L. Wang, Q. Wang, Aqueous photofate of crystal violet under simulated and natural solar irradiation: Kinetics, products, and pathways, Water Res., 88 (2016) 173-183.

Figure captions:

Figure 1: Scheme of electrochemical-cell with SPE.

Figure 2: Evolution of the concentration of 50 mg/L of CV in double distilled water during electrolysis at different applied currents. Conditions: stirring rate 800 rpm; T=20 °C; applied current: (✳) 0.5 A; (▦) 1 A and (⛆) 1.5 A.

Figure 3: Influence of the stirring rate on the evolution of the concentration of CV during treatment. Conditions: electrolyte: double distilled water; applied current 1 A; T=20 °C. stirring rate: (✳) 100 rpm; (▦) 400 rpm; (▤) 800 rpm; (⛆) 1100 rpm.

Figure 4: Influence of electrolyte on the evolution of the concentration of CV. Conditions: applied current 1 A; stirring rate 800 rpm; T=20 °C. Electrolyte: (×) double distilled water; (′) tap water; (π) 1g/L $NaHCO_3$; (✳) 0.6 g/L Na_2SO_4; (↵) 1 g/L Na_2SO_4.

Figure 5: Influence of the initial concentration of CV and temperature on the CV removal during the electrolysis. Conditions: applied current 1A; electrolyte: double distilled water; stirring rate: 800 rpm; CV concentration: (′) 25 mg/L, T = 20 °C; (□) 50 mg/L, T = 20 °C; (π) 100 mg/L, T = 20 °C; (×) 50 mg/L, T = 50 °C.

Figure 6: (a) Evolution of the (′) TOC, (π) CV concentration and (□) intermediates expressed as mg/L of carbon, during the electrolysis of 50 mg/L of CV. Conditions: stirring rate: 800 rpm; electrolyte: double distilled water; T =20 °C. The inset show the evolution of MCE. (b) Time course of the content of released (Δ) NH_4^+ and ($\leq$) NO_3^- in the same experiment.

Figure 7: Evolution of specific energy consumption with (π) TOC removal and (′) CV removal during oxidation of 50 mg/L of CV. Conditions: stirring rate: 800 rpm; electrolyte: double distilled water; T =20 °C.
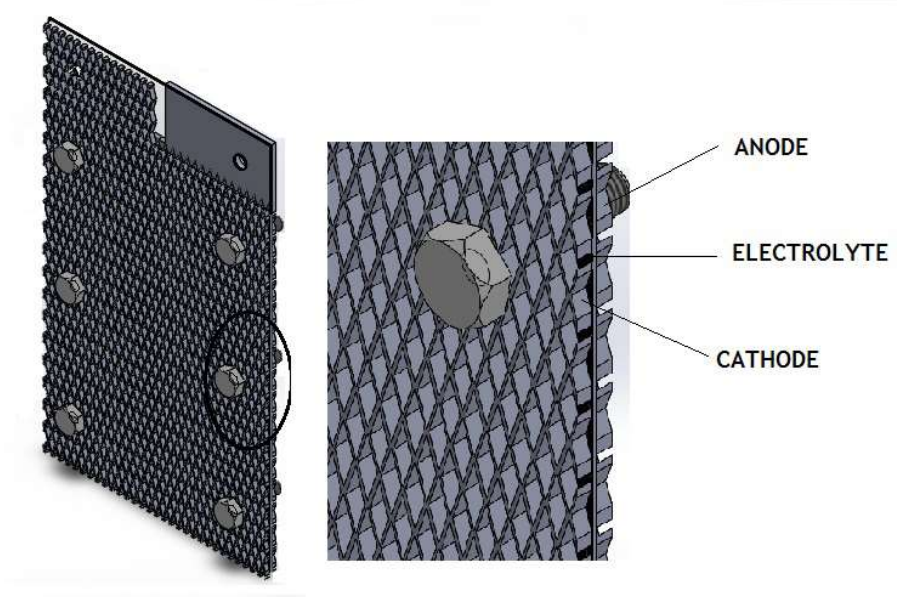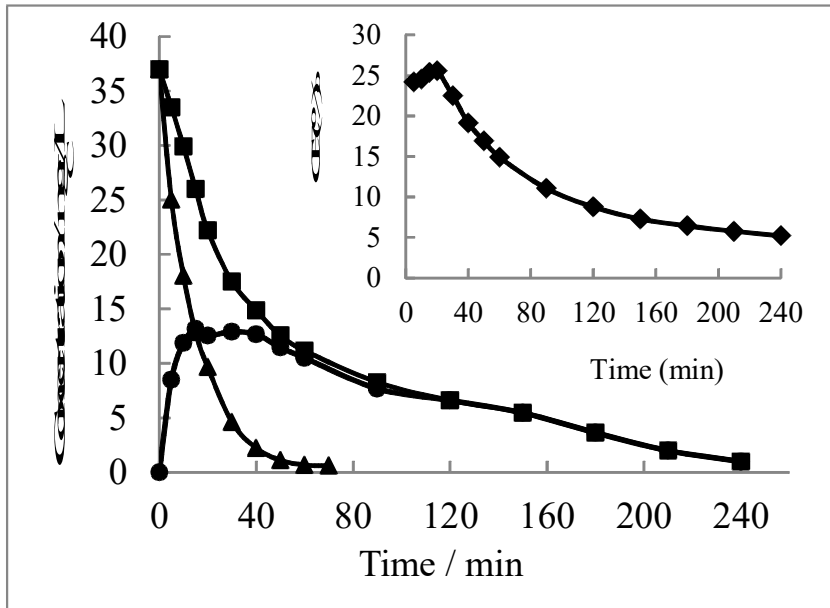
Labels: ANODE, ELECTROLYTE, CATHODE

FIGURE 1

FIGURE 2

FIGURE 3

FIGURE 4

FIGURE 5

Figure axes: Concentration / g L (y-axis), Time / min (x-axis). Inset: C (%) vs Time (min).

(a)

(b)

FIGURE 6

FIGURE 7